KeAi
CHINESE ROOTS
GLOBAL IMPACT

Available online at www.sciencedirect.com

ScienceDirect

Advances in Climate Change Research 11 (2020) 185−197

www.keaipublishing.com/en/journals/accr/

Mid-summer surface air temperature and its internal variability over China at 1.5 °C and 2 °C global warming

YIN Shu-Yue[a,b], WANG Tao[b,c,*], HUA Wei[a], MIAO Jia-Peng[c], GAO Yong-Qi[d], FU Yuan-Hai[c], Daniela MATEI[e], Evangelos TYRLIS[e], CHEN Dong[b]

[a] *Joint Laboratory for Climate and Environmental Change, Chengdu University of Information Technology, Chengdu, 610225, China*
[b] *Nansen-Zhu International Research Centre, Institute of Atmospheric Physics, Chinese Academy of Sciences, Beijing, 100029, China*
[c] *Climate Change Research Center, Chinese Academy of Sciences, Beijing, 100029, China*
[d] *Nansen Environmental and Remote Sensing Center, Bjerknes Center for Climate Research, Bergen, 5006, Norway*
[e] *Max Planck Institute for Meteorology, Hamburg, 20146, Germany*

Received 28 May 2020; revised 13 July 2020; accepted 8 September 2020
Available online 17 September 2020

Abstract

Recently, extremely hot summers occurred frequently across China, and the mean mid-summer surface air temperature (SAT) continuously broke the records of the past decades, causing huge social and economic losses. As global warming accelerates, these extremely hot summers will undoubtedly occur more frequently. However, the issue of what will happen to the mid-summer SAT over China in the near future remains unclear. Therefore, we investigate the changes of mid-summer SAT and related internal variabilities over China at 1.5 °C and 2 °C global warming above preindustrial level by using the MPI-ESM Grand Ensemble simulations. The results indicate that compared to the present-day (1986−2005), national averaged mid-summer SAT will increase by 1.1 °C and 2.0 °C, in 1.5 °C and 2 °C warming scenarios respectively. This means that the mid-summer SAT is projected to increase by 0.9 °C due to an additional 0.5 °C global warming, which is higher than the annual value (0.8 °C) and almost two times the global warming rate. Regionally, in the two warming targets, the increase in mid-summer SAT will be more enhanced over the northwestern part of China. In addition, the extremely high monthly SAT would increase nationwide due to an additional 0.5 °C in global warming. Among all areas, the Qinghai and Xinjiang provinces would experience the strongest increase in extremely high monthly SAT. It is important to find that, from 1.5 °C to 2 °C global warming, changes of the internal variability of the mid-summer SAT differs across China. It would decrease over some parts of western Northwest China, North China, Northeast China and the Tibetan Plateau. However, it would significantly increase over Qinghai, Sichuan, and northern parts of Inner Mongolia. As a result, at 2 °C global warming, the increase of extreme SAT in Qinghai is caused by the synergistic effect of stronger warming rate and larger internal variability. Differently, the increase in Xinjiang province is mainly caused by the stronger local warming. Further analysis suggests that we can effectively reduce the intensity of extremely hot months over most regions of Northwest China by limiting global warming to 1.5 °C, rather than to 2 °C.

Keywords: Mid-summer SAT; Internal variability; China; 1.5 °C global warming; 2 °C global warming

1. Introduction

Global warming has become an indisputable fact (e.g., Hansen et al., 2010; Kennedy et al., 2010; Qian et al., 2010; Wang et al., 2013; Thorne, 2015). From 1906 to 2005, the global average surface temperatures increased by approximately 0.74 °C (Trenberth et al., 2007). Different regions are warming at different rates, with more warming over land than

* Corresponding author. Nansen-Zhu International Research Centre, Institute of Atmospheric Physics, Chinese Academy of Sciences, Beijing, 100029, China.
E-mail address: wangtao@mail.iap.ac.cn (WANG T.).
Peer review under responsibility of National Climate Center (China Meteorological Administration).

https://doi.org/10.1016/j.accre.2020.09.005

the ocean, and especially over the high latitudes of the Northern Hemisphere (e.g., Hansen et al., 2006; Sutton et al., 2007; Thorne, 2015). If we do not restrict emissions, in the 21st century, global surface temperatures are expected to continue to rise (e.g., Knutti et al., 2008; Fu et al., 2011; Joshi et al., 2011; Zhang, 2012; Zhang et al., 2013; Wang and Yang, 2014; Jiang et al., 2016; Karmalkar and Bradley, 2017; Chen et al., 2019). Recently, studies based on the Coupled Model Intercomparison Project Phase 5 (CMIP5) have shown that the global average surface temperature is projected to reach 1.5 °C above the preindustrial levels in 2036, 2028 and 2025 under RCP2.6, RCP4.5 and RCP8.5 scenarios in multimodel ensemble, respectively (e.g., Hu et al., 2017; Xu et al., 2017). The global average surface temperature is projected to reach 2 °C above the preindustrial levels in 2049 and 2039 under RCP4.5 and RCP8.5, respectively, and even reach 4 °C in 2081 under the RCP8.5 scenario (Hu et al., 2017; Zhai et al., 2017; Wang et al., 2018b). Schneider et al. (2007) noted that global warming of 2−4 °C, relative to that in 1990−2000, will lead to a reduction in biodiversity and crop productivity, glacial ablation of the Greenland and West Antarctica ice sheets, etc.

Therefore, the long-term goal of the Paris Agreement was set to "hold the increase in the global average temperature to well below 2 °C above preindustrial levels and pursuing efforts to limit the temperature increase to 1.5 °C" (UNFCCC, 2015). A recent modeling study suggests that the intensity, frequency and duration of the extreme heat events are projected to increase over China from stabilized 1.5−2 °C global warming (Zhang et al., 2020). In many regions of the world, for an additional 0.5 °C of global warming, extreme temperatures will also significantly increase (Wang et al., 2017b; Dosio et al., 2018; Wehner et al., 2018; Sun et al., 2019). For example, the frequency of hot summer in Europe will increase by at least 24% (King and Karoly, 2017), and the intensity, frequency and duration of extreme high temperature events will increase by 35%−46% over East Asia (Li et al., 2018a). On the contrary, the occurrence of the winter extreme low temperature decreases significantly over the Northern Hemisphere (Kuang et al., 2019).

In China, annual and seasonal surface air temperature (SAT) is both projected to increase with global warming (e.g., Lang and Sui, 2013; Zhou et al., 2014, 2016a; Wang et al., 2017a; Zhou et al., 2019a; Miao et al., 2020). However, the increases are different across the country, with the northwestern region warming fastest and being higher than the global average (e.g., Jiang et al., 2009; Xu and Xu, 2012; Lang and Sui, 2013; Hu et al., 2017; Fu et al., 2018). For an additional 0.5 °C of global warming, the annual mean SAT is expected to increase by 0.7 °C (Chen and Sun, 2018), and the summer SAT will rise by approximately 0.7 °C under the RCP4.5 scenario and 0.8 °C under the RCP8.5 scenario (Zhou et al., 2019a). The temperature extremes over most regions of China are also projected to increase more than 0.5 °C under the RCP4.5 and RCP8.5 scenarios (Shi et al., 2018). In addition, from 1.5 °C to 2 °C global warming, extreme precipitation events over China is projected to increase by nearly 4% (Li et al., 2018b), and the incidence of drought and extreme drought is projected to increase by approximately 9% and 8%, respectively (Chen and Sun, 2019).

In fact, research on the effects that could be avoided by stabilizing global warming at 1.5 °C rather than 2 °C is still lacking (e.g., Mitchell et al., 2016; Rogelj and Knutti, 2016; Schleussner et al., 2016; Zhai et al., 2017). A number of studies have focused on the change in mean climate and extreme events (e.g., Jiang et al., 2004; Xu et al., 2005; Gao et al., 2013; Lang and Sui, 2013; Zhang et al., 2020). However, how climate variability responds to an additional 0.5 °C of global warming and its impacts on mean and extreme climates are still unclear. On the other hand, in recent years, China has frequently experienced extremely high temperatures in mid-summer (July and August), which has reduced crop yields and affected human health (e.g., Hou et al., 2014; Sun et al., 2014; Zou et al., 2015; Chen et al., 2016; Xu et al., 2019). Issues such as how hot the mid-summer will be in China in the near future are getting more and more attention. Therefore, we investigate changes in mid-summer SAT over China at 1.5 °C and 2 °C global warming based on the Max Planck Institute Earth System Model (MPI-ESM) Grand Ensemble. In this ensemble, there are 100 realizations for both the historical and future warming experiments. The size of the ensemble is largest in the current same type of simulations, which can be used to robustly identify the internal variability in a changing climate (Suárez-Gutiérrez et al., 2018). Thus, changes in mid-summer SAT internal variability and their possible contributions to the extreme SAT at the above-mentioned two warming targets are also examined. This study is to highlight the importance of limiting global warming to 1.5 °C for reducing extreme high mid-summer SAT over China.

2. Data and methods

Transient simulations from the MPI-ESM Grand Ensemble, which include monthly output derived from the historical experiment (1850−2005) and two RCP scenario experiments (RCP2.6 and RCP4.5, 2006−2099), are analyzed. The MPI-ESM Grand Ensemble uses the model MPI-ESM version 1.1 (Suárez-Gutiérrez et al., 2018). The model is run with resolution T63, and a total of 47 vertical levels are employed in the atmosphere. In the oceanic component, the resolution is 1.5° and 40-level on the horizontal and vertical directions, respectively. In each experiment, there are 100 realizations. They are all forced by the same external agents but with different initial climate states. In addition, monthly observational data from the CN05.1 dataset (Wu and Gao, 2013) are also used to assess the model results and to quantify the observed high SAT records.

There are many methods that can be used to define a 1.5 °C and 2 °C warming world (e.g., King et al., 2017; Wang et al., 2018a; Wang et al., 2018b). In this study, we set the ensemble mean of 100-realization simulated global mean SAT during the period of 1851−1880 as the preindustrial level, with standard deviation of 0.13 °C. We use the same method as Suárez-Gutiérrez et al. (2018) to construct representative

samples of the 1.5 °C and 2 °C warming scenarios. Based on the 9-year running averages, the years in which the global mean SAT is in the range of 1.5/2 ± 0.13 °C above the pre-industrial level are taken as samples of 1.5/2 °C global warming. This selection can reduce the influences of decadal variabilities on the global warming projections (Suárez-Gutiérrez et al., 2018). In addition, we use all the years during 1986–2005 from the 100 historical realizations as the present-day sample, which is used as a reference sample. The analyzed changes in SAT and associated internal variability are based on the differences between 1.5/2 °C and present-day or between 1.5 °C and 2 °C. The simulated preindustrial climate is only used to construct the 1.5 °C and 2 °C global warming.

We mainly investigate changes in mid-summer SAT over China and subregions for the two global warming targets. A standard *t* test is used to determine the statistical significances. In addition, related internal variability is examined, which is measured as the difference between the 97.5th and 2.5th percentiles. Finally, we further investigate the SAT for extremely hot months with return periods of 20 years and 100 years to assess the possible changes in extremely high temperature from 1.5 °C to 2 °C of global warming. The return periods of 20 and 100 years indicate that the expected probability of the event happening in a given period are 1/20 (i.e., 5%) and 1/100 (i.e., 1%), respectively. The Gumbel distribution, based on probability weighting moments, is used to calculate the return values because it is suitable for investigating the extreme temperatures in different regions of China (Ding et al., 2004).

3. Results

As shown in Fig. 1, there are ~5900 under the RCP2.6 scenario and ~1359 model years under the RCP4.5 scenario that satisfy the 1.5 °C threshold. For the 2 °C threshold, there are no model years under the RCP2.6 scenario and ~2900 model years under the RCP4.5 scenario. Therefore, we choose these ~2900 model years under the RCP4.5 scenario, which satisfy the 2 °C threshold, to construct the sample of 2 °C global warming. Then, we only choose the years satisfying these conditions during 2051–2080 under the RCP2.6 scenario (i.e., ~2900 model years) as the 1.5 °C samples to ensure the number of years is similar to that for the 2 °C world. Thus, we can avoid the possible impacts of different sample sizes of the two warming targets on the study.

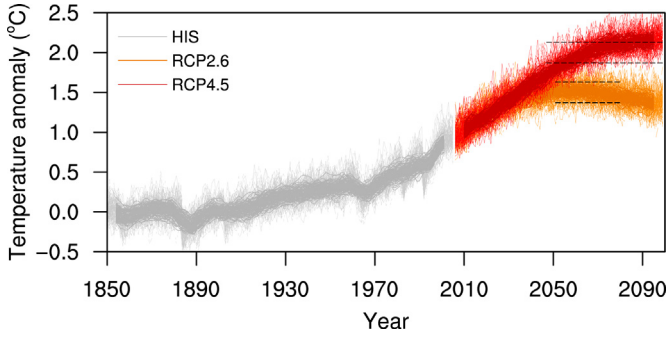

Fig. 1. Time series of annually global mean SAT anomalies and 9-year moving averages of the global mean SAT for 1850–2099. Simulations include output derived from the historical experiment (HIS) over 1850–2005, RCP2.6 and RCP4.5 scenarios experiments over the period of 2006–2099. The black dashed lines represent the periods of sampling for 1.5 °C and 2 °C global warming (modified from Fig. 1, Suárez-Gutiérrez et al. (2018)).

3.1. Mid-summer SAT over China

Figure 2a shows simulated probability distributions of the global annual mean SAT anomalies in the three climates. In the present-day climate, the global mean SAT is 14.4 °C, with a distribution width of 1.2 °C. In contrast, the widths of the 1.5 °C and 2 °C distributions are relatively narrow, at 0.8 °C and 1.0 °C, respectively. At 1.5 °C global warming, the global mean SAT increases by 0.8 °C. Correspondingly, the simulated 2 °C global warming has a global mean SAT that increases by 1.3 °C, which is 0.5 °C higher than that of the 1.5 °C global warming. In addition, the 1.5 °C distribution overlaps approximately 1% of its area with the present-day distribution, and it overlaps approximately 5% of its area with the 2.0 °C distribution. This means that more than 90% of the SATs can be distinguished from each other at a global scale.

Over China, the simulated regionally-averaged annual mean SAT for 1986–2005 is 6.5 °C, which is very close to the observed annual mean SAT (6.7 °C, CN05.1 dataset). Compared with the global distributions, those over China are wider, and the 1.5 °C and 2 °C distributions move towards higher SAT anomalies (Fig. 2b). The results show that in comparison to that at the present-day, the annual mean SAT in 1.5 °C global warming increases by 1.2 °C, and that in a 2 °C world increases by 2.0 °C. The additional 0.5 °C of global warming results in a further increase of 0.8 °C over China, suggesting a higher warming rate than the global average rate over China. At the same time, the corresponding widths of the SAT anomaly distributions are 2.9 °C, 2.2 °C and 2.6 °C for the present-day and two warming climates. These values are all more than twice the global mean, suggesting greater internal variability occurs at the regional scale, as noted by Suárez-Gutiérrez et al. (2018). Therefore, the simulated distributions of the annual mean SAT anomalies over China for the present-day and two warming climates show increased overlap in area (~9% for the present-day and the 1.5 °C global warming and ~23% for the 1.5 °C and 2 °C global warming). There are even some overlaps between the present-day and the 2 °C global warming. However, most of the SAT anomalies are significantly distinguishable from each other. This means that over China, more than 90% of the annual mean SAT in 1.5 °C global warming is higher than that at the present-day. Furthermore, nearly 80% of the annual mean SAT in 2 °C global warming is higher than that in 1.5 °C global warming.

We focus on the future evolution of mid-summer SAT over China in the two warming climates, particular on the internal variability. Thus, we firstly evaluate the ability of the MPI-ESM Grand Ensemble in simulating the modern mid-summer SAT over China. As shown in Fig. 3a, the model can well reproduce the observed distributions of averaged mid-summer SAT over China. To investigate regional changes

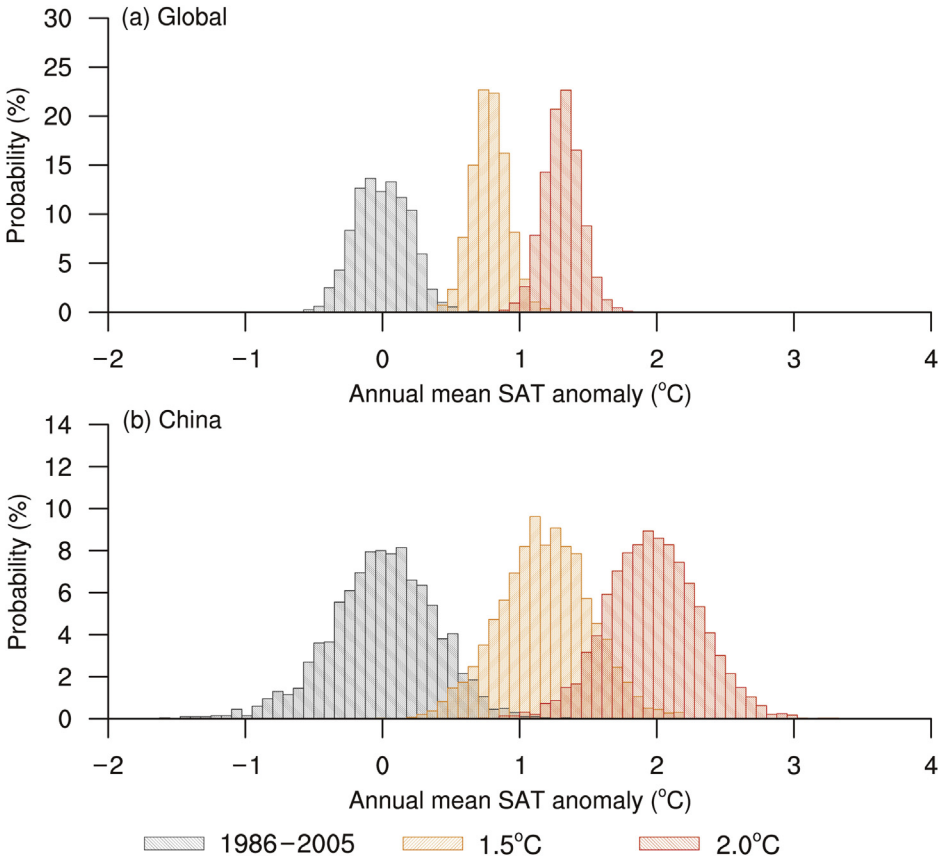

Fig. 2. Simulated probability distributions of annual mean SAT anomalies relative to 1986–2005 at different global warming targets, (a) global, (b) China (Bin size is 0.075 °C).

of mid-summer SAT over China in the two warming climates, we divide China into nine subregions referring to Yao et al. (2017) and Xu et al. (2018). The subregions are western Northwest China, eastern Northwest China, North China, Northeast China, Tibetan Plateau, Central China, East China, Southwest China, South China (more detailed information can be found in Fig. 5a). This division can fully consider different responses of SAT over China to climate change (Chen et al., 2015).

As shown in Fig. 3b–j, comparison between simulation and observation indicates a good agreement in the distribution of regional averaged mid-summer SAT over China. Only one or two observed mid-summer SATs occur outside of the simulation in East China (Fig. 3f) and Central China (Fig. 3g). Further statistics show that the MPI-ESM Grand Ensemble can simulate the averaged mid-summer SAT anomalies over China and the nine subregions during the present-day (Table 1). Overall, the evaluation indicates that the MPI-ESM Grand Ensemble is able to offer an adequate representation of the estimated variability over China and the nine subregions, which is a good starting point to address the following projection.

The simulated distributions of mid-summer SAT anomalies over China for the present-day and two warming climates are similar to the annual distributions (Fig. 4a). The statistics show that over China (Table 1), compared with that at the present-day, the regionally averaged mid-summer SAT in 1.5 °C global warming increases by 1.1 °C and that in 2 °C global warming increases by 2.0 °C. The additional 0.5 °C global warming can lead to an increase of 0.9 °C in the mid-summer SAT over China, which is slightly higher than the annual SAT (0.8 °C). The corresponding widths of the mid-summer SAT anomaly distributions are all 2.6 °C for the present-day, 1.5 °C global warming and 2 °C global warming. In 1.5 °C global warming, more than 53% of the mid-summer SATs would be higher than the observed hottest record (1.1 °C above the present-day) during 1961–2018. This means that every other mid-summer will be hotter than the present hottest record. Even worse, almost all mid-summers would be hotter under 2 °C global warming.

3.2. Mid-summer SAT over the subregions

Spatially, mid-summer SATs increase significantly over all of China in 1.5 °C global warming in comparison with that at the present-day, and these SATs increase more strongly in 2 °C global warming (Fig. 5a and c). Additionally, the spatial differences in the mid-summer SATs manifest as an increase from south to north and even from east to west, which is similar to the results of previous studies (e.g., Jiang and Fu, 2012; Xu et al., 2017; Wang et al., 2018a). This kind of spatial characteristic is particularly notable at 2 °C global

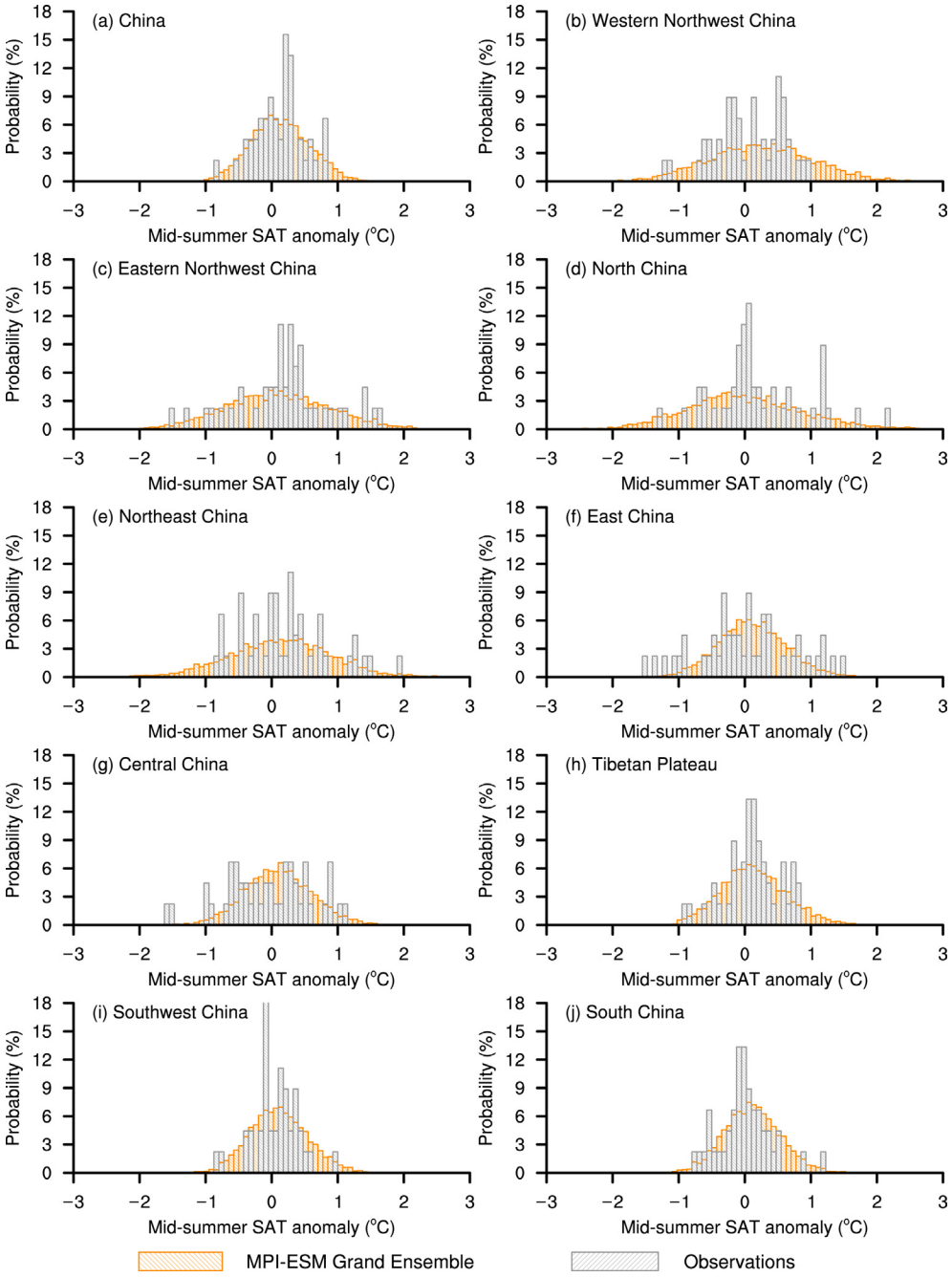

Fig. 3. MPI-ESM Grand Ensemble simulated and observed distributions of mid-summer SAT anomalies relative to 1961−1990 over (a) China, and the nine subregions (b−j) for the period of 1961−2005 (Bin size is 0.075 °C).

warming. With respect to the present-day, the increases in the mid-summer SAT range are from 0.7 to 1.4 °C and from 1.2 to 2.8 °C for the 1.5 °C and 2 °C global warming, respectively. An additional 0.5 °C global warming would lead to an increased SAT ranging from 0.5 to 1.5 °C in the mid-summer over China (Fig. 5e). Especially in western Northwest China and eastern Northwest China, the additional increases in mid-summer SAT from 1.5 °C to 2 °C global warming are greater than 1.0 °C and even reach as high as 1.5 °C over the western Northwest China (Fig. 5e), which indicates that the warming over these two regions are greater (2−3 times) than the national average. The regionally averaged mid-summer SAT anomalies are 1.3 °C for western Northwest China and 1.4 °C for eastern Northwest China at 1.5 °C global warming. At 2 °C global warming, the averaged mid-summer SAT anomalies are 2.6 °C and 2.5 °C for western Northwest China and eastern Northwest China, respectively. The western Northwest China has the greatest increase in warming in 2 °C global warming, while the eastern part of the eastern Northwest China has the greatest increase in 1.5 °C global warming.

In addition, the simulated probability distributions of the mid-summer SAT anomalies for the western Northwest China

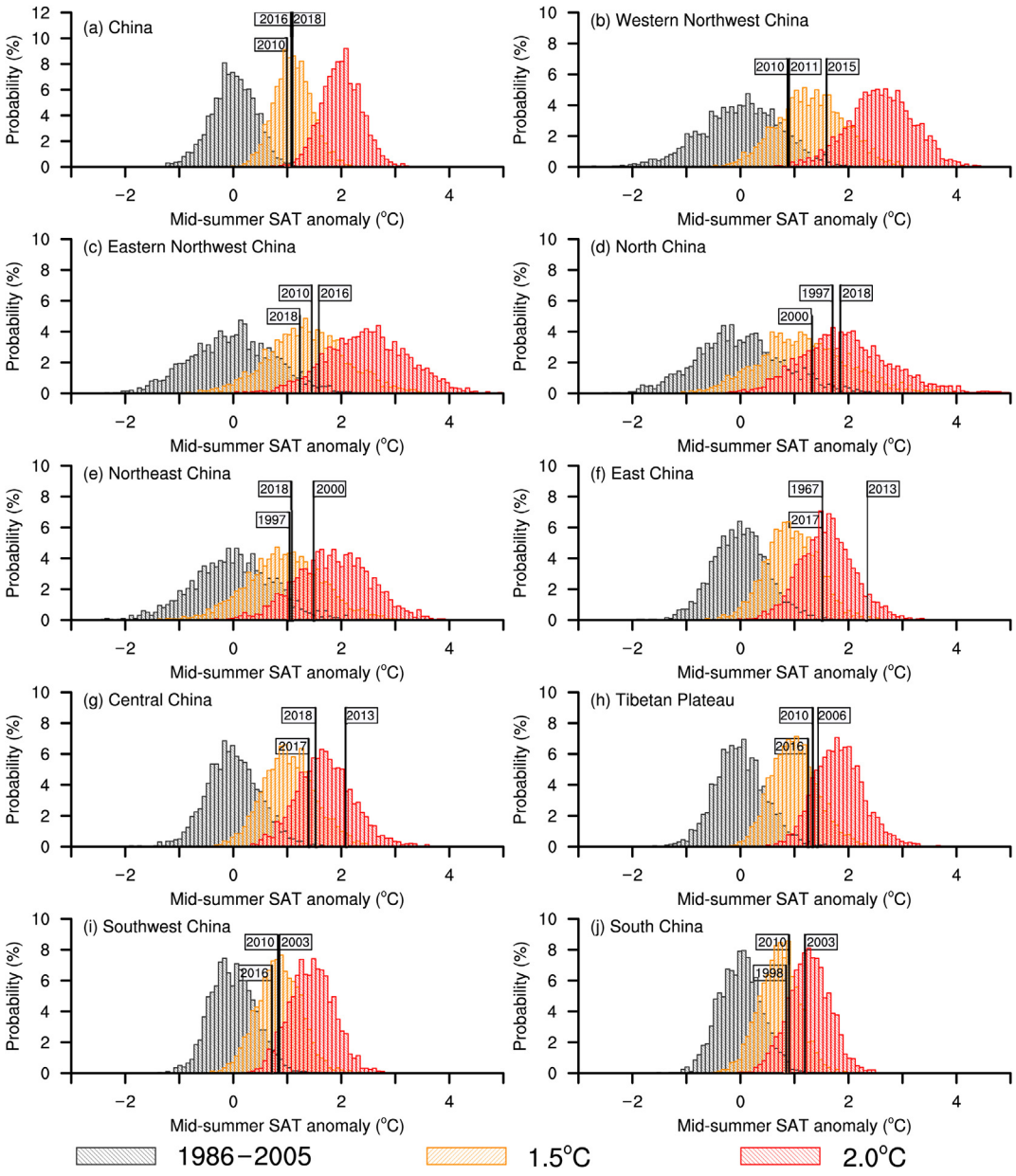

Fig. 4. Simulated probability distributions of mid-summer SAT anomalies relative to 1986−2005 over (a) China and (b−j) the nine subregions. The black reference lines represent the three largest mid-summer SAT anomalies in each region during 1961−2018 (Bin size is 0.075 °C).

and eastern Northwest China are also different from the national-averaged distributions (Fig. 4) as they present widths almost two times greater than those of the national-averaged distributions, implying a greater internal variability of regional climates. Additionally, compared with the whole China and other subregions, the western Northwest China and eastern Northwest China mid-summer SAT anomaly distributions for both warming climates shift towards higher SAT anomalies. The areal overlaps between 1.5 °C and 2 °C distributions are approximately 30% and 45% for the western Northwest China and eastern Northwest China, respectively, which are lower relative to those of the other subregions, except for the Tibetan Plateau. These results indicate that approximately 70% of the western Northwest China mid-summers and more than half of the eastern Northwest China mid-summers in 2 °C global warming would be distinguishable from those in 1.5 °C global warming. The results also further confirm maximum warming over these two regions in 1.5 °C global warming and specifically in 2 °C global warming. Compared with the observations, the simulations show that every three mid-summers over eastern Northwest China and western Northwest China in 1.5 °C global warming would be warmer than the hottest record. In 2 °C global warming, the percentage of relatively hotter mid-summers increases to 88% and 95% over eastern Northwest China and western Northwest China, respectively.

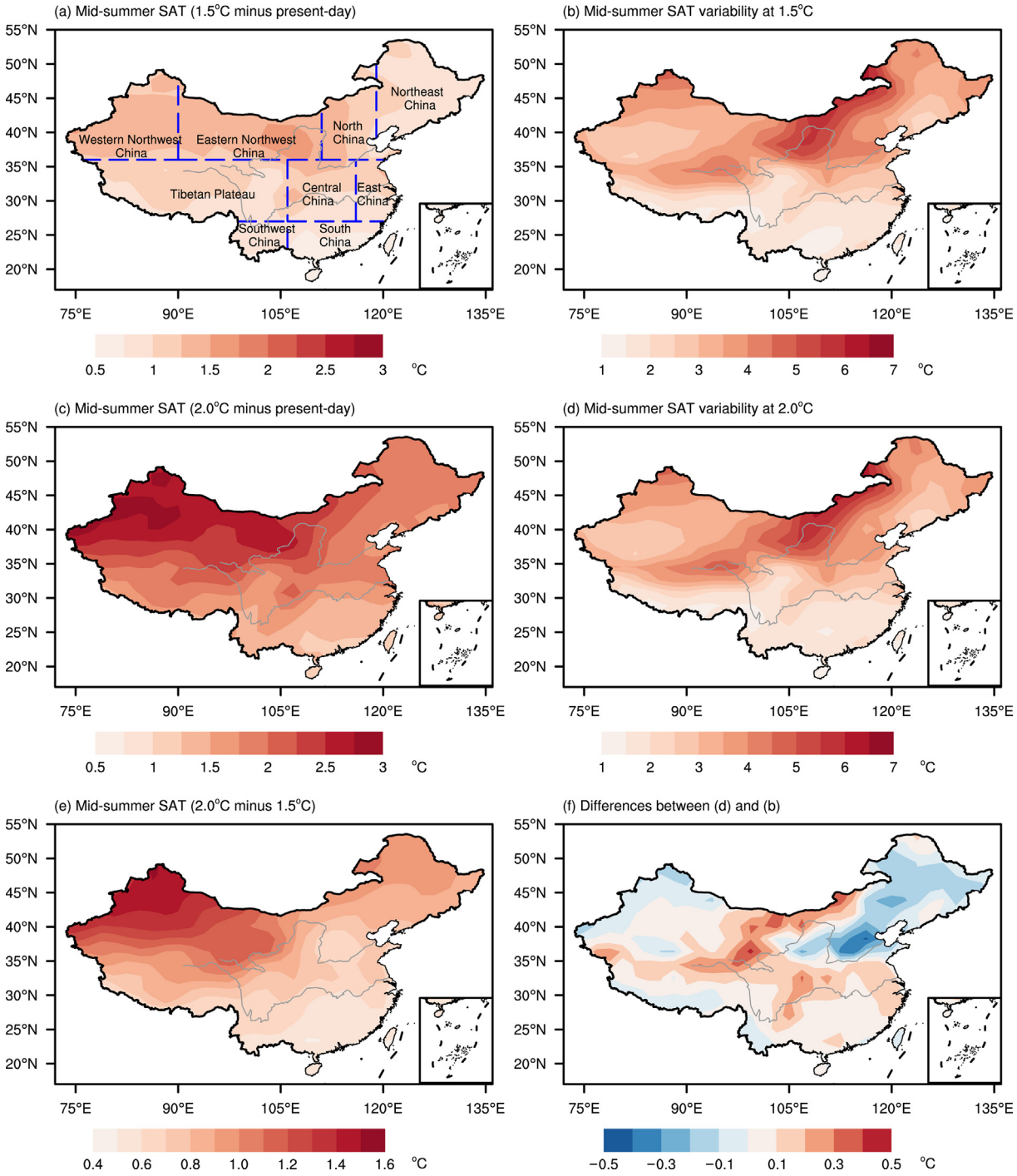

Fig. 5. Mid-summer SAT changes and variability at 1.5/2.0 °C global warming targets, (a) differences in mid-summer SAT (1.5 °C global warming minus present-day), (b) mid-summer SAT variability at 1.5 °C global warming, measured as the difference between 97.5th minus 2.5th percentiles, (c) differences in mid-summer SAT (2 °C global warming minus present-day), (d) mid-summer SAT variability at 2 °C global warming, as in (b), (e) differences in mid-summer SAT at 2 °C global warming minus 1.5 °C global warming, and (f) differences in mid-summer SAT variability (2 °C global warming minus 1.5 °C global warming) (In (a), (c) and (e), all the areas exceed 95% confidence level).

In fact, the North China and Northeast China mid-summer SAT anomaly distributions are also relatively wider, similar to those of eastern Northwest China and western Northwest China (Fig. 4d and e). They are centered around the 1 °C anomaly in 1.5 °C global warming and around the 2 °C anomaly in 2 °C global warming, indicating a moderate warming rate between the northwestern regions and other subregions (also shown in Fig. 5a and c). When comparing North China and Northeast China, warming in the former is greater in both warming climates (Fig. 5a and c). In 1.5 °C and 2 °C global warming, the regionally averaged mid-summer SAT anomalies over North China are 1.2 °C and 2.0 °C,

Table 1
Observed and simulated regionally-averaged mid-summer SAT anomaly (unit: °C, relative to 1961−1990) over China and the nine subregions during the present-day (1986−2005) and simulated changes in 1.5 °C and 2 °C global warming.

Region	Observed present-day anomaly	Simulated present-day anomaly	1.5 °C minus present-day	2 °C minus present-day
China	0.3	0.4	1.1	2.0
Western Northwest China	0.2	0.6	1.3	2.6
Eastern Northwest China	0.5	0.3	1.4	2.5
North China	0.4	0.0	1.2	2.0
Northeast China	0.5	0.4	1.0	1.9
East China	−0.1	0.3	1.0	1.6
Central China	−0.2	0.3	1.1	1.7
Tibetan Plateau	0.3	0.4	1.0	1.8
Southwest China	0.1	0.3	0.9	1.5
South China	0.0	0.3	0.7	1.3

respectively, which are greater than the values of 1.0 °C and 1.9 °C over Northeast China. The areal overlaps between the 1.5 °C and 2 °C distributions are 63% and 52% for North China and Northeast China, respectively. They are the largest values among those of the subregions. This result indicates that the relatively fewer mid-summer SATs over North China and Northeast China, compared with those over other subregions, in 2 °C global warming would be distinguishable from those in a 1.5 °C world. The observed hottest mid-summer over North China occurred in 2018, when the observed mean SAT anomaly was 1.9 °C. It was the largest observed mid-summer SAT anomaly over the northern four subregions. At 1.5 °C and 2 °C global warming, 22% and 55% of the mid-summers, respectively, will be hotter than that in 2018. For Northeast China, the observed largest mid-summer SAT anomaly was 1.5 °C in 2000. In the two warming climates, approximately 24% and 72% of the mid-summers, respectively, would be hotter than this hottest record.

Over East China, Central China, Tibetan Plateau, Southwest China, and South China, the widths of the mid-summer SAT distributions for the present-day and two warming climates are narrower compared with those of the other four subregions (Fig. 4f−j). Specifically, over South China, the widths are narrowest. These results indicate relatively smaller internal variability of three climates over these regions. At the same time, the warming over these subregions is also weaker in 1.5 °C and 2 °C global warming (Fig. 5 and Table 1). Over the Tibetan Plateau, the areal overlap between the 1.5 °C and 2 °C distributions is approximately 35%, suggesting that more than 60% of the mid-summers in 2 °C global warming would be distinguishable from those in 1.5 °C global warming. This result is similar to the situation for western Northwest China. Differently for the other four subregions, areal overlaps between the 1.5 °C and 2 °C distributions range from 45% to 51%, indicating that approximately half of the mid-summers in 2 °C global warming would be distinguishable from those in 1.5 °C global warming.

Among these five subregions (East China, Central China, Tibetan Plateau, Southwest China, and South China), the observed largest mid-summer SAT anomaly was 2.4 °C in 2013 (Fig. 4f), which is 0.9 °C higher than the second largest anomaly in 2017. This anomaly is also the largest regional record over China. In contrast, the MPI-ESM could not reproduce such hot mid-summer over the East China at the present-day. Even in 1.5 °C and 2 °C global warming, only 0.4% and 8% of the mid-summers, respectively, would be hotter than that in 2013. The hottest mid-summer over Central China was also observed in 2013 (Fig. 4g), with the largest anomaly of 2.1 °C. In 1.5 °C and 2 °C global warming, approximately 3% and 24% of the mid-summers, respectively, would be hotter than that in 2013. Over the Tibetan Plateau, Southwest China and South China, the observed largest mid-summer SAT anomalies are relatively smaller (Fig. 4h−j), 1.4 °C in 2006, 0.9 °C and 1.2 °C in 2003, respectively. In 1.5 °C and 2 °C global warming, there would be 50% and 93% of mid-summers, respectively, hotter than the observed hottest record over Southwest China. For the Tibetan Plateau, 15% and 79% of the mid-summers would be hotter in 1.5 °C and 2 °C global warming, respectively, than that in the observed record.

Figure 5b and d shows the spatial patterns of mid-summer SAT internal variability in 1.5 °C and 2 °C global warming, which more clearly illustrate the regional differences in internal variability. These results indicate large SAT internal variabilities over northern parts of China with particularly larger internal variabilities over eastern Northwest China and North China. These variabilities correspond well to the wider mid-summer SAT distributions for the four northern subregions. The two spatial patterns at 1.5 °C and 2 °C global warming are similar, suggesting inherent characteristics of regional internal variability. However, the impact of global warming on this inherent internal variability cannot be ignored. As shown in Fig. 5f, due to an additional 0.5 °C of global warming, the mid-summer SAT internal variability decreases over North China, Northeast China and the western parts of western Northwest China and Tibetan Plateau, whereas it increases over other regions. Among the regions with increased internal variability, changes in Qinghai, Inner Mongolia, and Sichuan provinces are the most notable, suggesting possibly more extremely hot mid-summers there from 1.5 °C to 2 °C global warming. On the contrary, the number of extremely hot mid-summers may be reduced over North China, Northeast China and areas with decreased internal variability in 2 °C global warming.

3.3. Extremely high monthly SAT over China

Due to the limitations of monthly data, we investigated changes in extremely high monthly SAT for events with return periods of 20 and 100 years at 1.5 °C and 2 °C global warming. As shown in Fig. 6a–d, the spatial patterns of extreme SATs are similar for different return periods and global warming levels. The highest SATs occur over western Northwest China, and the lowest SATs occur over the Tibetan Plateau. The extreme SATs are also relatively higher over the Shandong Peninsula and adjacent areas. The differences in the 20-year return levels between 1.5 °C and 2 °C global warming are similar to changes in mid-summer SAT from the 1.5 °C to 2 °C global warming (Fig. 6e), showing larger anomalies towards the northwest than towards the other directions. The differences are largest in the Qinghai and northern Xinjiang provinces, with values close to 1.5 °C. However, differences are smaller over North China and Southwest China. These results indicate that the increase in the extremely high SAT is the strongest in the Qinghai and northern Xinjiang provinces but the weakest over North China and Southwest China. The 100-year return levels also exhibit the same feature (Fig. 6f) but suggest a stronger increase in extremely high SAT in Qinghai from 1.5 °C to 2 °C global warming. The value of the strongest increase is larger than 1.5 °C.

We further investigated the differences between changes in extreme SAT and changes in mid-summer SAT. As shown in Fig. 6g and h, the spatial patterns resemble the differences in the mid-summer SAT internal variability between the 2 °C and 1.5 °C global warming. This result suggests that increasing internal variability is one of the most important causes of the increase in extreme SAT from 1.5 °C to 2 °C global warming. Therefore, the increase in the extreme SAT is stronger than that of the mid-summer SAT in Qinghai, Inner Mongolia, and southern parts of China. Particularly for the greatest increase in extreme SAT in Qinghai province, it is caused by the synergistic effect of a relatively stronger warming and greater internal variability. Differently, another greatest increase in extreme SAT in Xinjiang province is mainly caused by its highest local warming.

4. Discussion

We quantified changes of mid-summer SAT over China and the nine subregions between the two warming targets for 2006–2099. It shows that in the 2 °C global warming, approximately 80% of the mid-summers over China would be distinguishable from those in 1.5 °C global warming. In 1.5 °C global warming, the high SAT such as the observed hottest record (1.1 °C in 2018) is projected to become normal, while in 2 °C global warming, almost all mid-summers would be hotter than that.

Across China, the SAT rise is different. The warming is the strongest over the Northwest China in the two warming climates. Zhou et al. (2015, 2016b) found that the warming rate over land between 50 °S and 50 °N during 1979–2012 intensified with the decrease of the vegetation greenness on the land, especially in the driest regions. In addition, they found that this may be mainly attributed to the increase in longwave radiative forcing, which is related to stronger water vapor feedback over drier ecoregions in response to the positive global-scale greenhouse gas forcing. As a result, the warming rate in the Northwest China, where are arid and semi-arid regions, is relatively stronger.

We also examined the internal variability of mid-summer SAT at the two warming targets. Differently from changes of mid-summer SAT, internal variability decreases over North China, Northeast China and the western parts of western Northwest China and Tibetan Plateau from 1.5 °C to 2 °C global warming, whereas increases over other regions. In fact, the reason of different changes in internal variability is unclear. Based on Yu et al. (2020), internal variability is the result of intrinsic processes in the climate system, especially the coupling interactions between the atmosphere, ocean, land and cryosphere, and these interactions have different effects on each region. For China, the underlying surface of the terrain is complex and the regional differences are very large. Therefore, the different thermal and dynamic processes over regions can lead to different internal variability.

In this study, we mainly analyzed changes in mid-summer SAT at 1.5 °C and 2 °C global warming. So at a longer time scale in the future, how will the mid-summer SAT change over China? Thus, we calculated the linear trends in mid-summer SAT under both RCP 2.6 and RCP 4.5 scenarios throughout the 21st century (Table 2). The linear trend is 0.06 °C per decade under the RCP 2.6 scenario over China; under the RCP 4.5 scenario, the linear trend is close to 4 times of that under the RCP2.6 scenario. Among subregions, the linear trends in mid-summer SAT are different. Under the RCP 4.5, greater linear trends can be found in northern regions of China, particularly in Northwest China. It further suggests that the Northwest China will experience stronger warming and extreme high SAT in the future.

The increase in mid-summer SAT indicates that the intensity and frequency of extreme high temperature may increase, which can increase electricity consumption (Zhang and Wang, 2002; Li et al., 2020), crops loses (Zhang et al., 2011; He, 2017; Zhou et al., 2019b), and cause serve economic losses (Kilbourne, 1997; IPCC, 2012; Qin et al., 2015). For instance, high temperatures occurred in eastern China in the summer of 2013, followed by drought, causing an estimated 59 billion RMB in economic losses (Hou et al., 2014; Sun et al., 2014). The 2014 drought in California has broken records in many places, causing a large area of crop losses and leading to total economic costs estimated at 2.2 billion USD (Howitt et al., 2014; Swain et al., 2014; Williams et al., 2015). Moreover, extreme heatwaves even threaten human health (Díaz et al., 2002; Gosling et al., 2008; Robine et al., 2008), thus reducing the labor productivity (Kjellstrom and Crowe, 2011; Su et al., 2018; Yu et al., 2019). In the summer of 2003, a record high temperature in Europe was estimated to have caused more than 70,000 casualties (Robine et al., 2008). Our results suggest that from 2 °C to 1.5 °C global warming, the intensity of extremely hot months over China, especially over Northwest China, can be effectively reduced. Therefore,

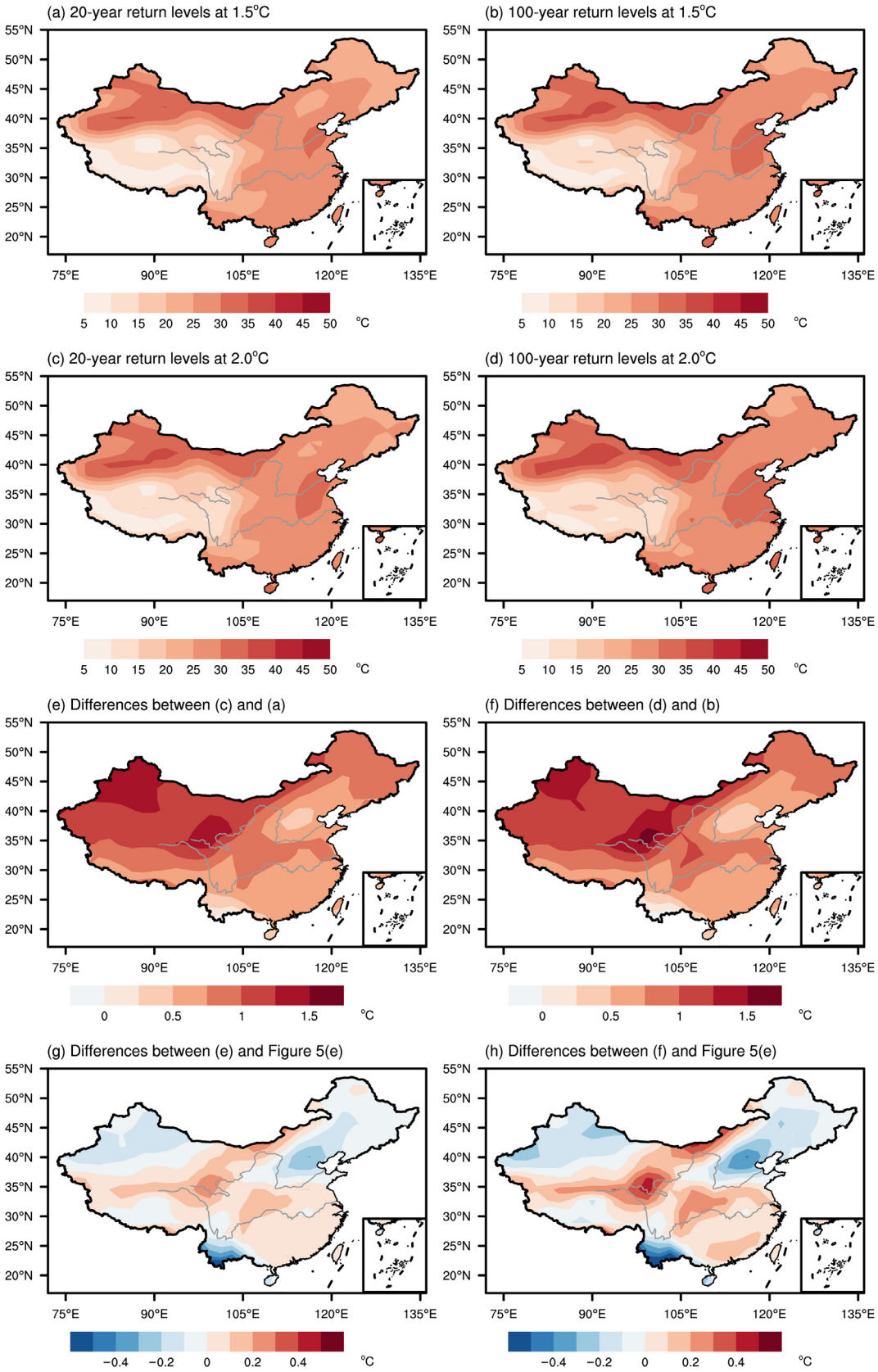

Fig. 6. Extreme high monthly SAT for events with (a) 20-year and (b) 100-year return periods at 1.5 °C global warming, (c) 20-year and (d) 100-year return periods at 2 °C global warming, (e) differences in extreme high monthly SAT for events with 20-year return periods between 2 °C and 1.5 °C global warming, (f) same as (e), but for events with 100-year return periods, (g) differences between Figs. 6e and 5e, and (h) differences between Figs. 6f and 5e.

Table 2
Regionally-averaged linear trends in mid-summer SAT over China and nine subregions under the RCP 2.6 and RCP 4.5 scenarios during 2006−2099 (unit: °C per decade).

Region	RCP2.6	RCP4.5
China	0.06	0.23
Western Northwest China	0.03	0.27
Eastern Northwest China	0.08	0.30
North China	0.11	0.27
Northeast China	0.04	0.21
East China	0.05	0.17
Central China	0.07	0.19
Tibetan Plateau	0.04	0.20
Southwest China	0.04	0.16
South China	0.04	0.14

it is very important to limit global warming to 1.5 °C, which can significantly reduce various risk in the future over China.

As mentioned above, the MPI-ESM Grand Ensemble can well reproduce the observed regionally averaged mid-summer SAT anomalies. At the national scale, the model bias is only 0.1 °C (Table 1). However, for some subregions, the model uncertainties are larger, such as 0.4 °C in western Northwest China and −0.4 °C in North China. It is difficult to examine whether the model uncertainties will change with global warming and thereby possibly have an impact on the present analysis. At the same time, the present results are based on the output derived from the MPI-ESM. It is necessary to note that the results are likely to have model dependence. Therefore, large ensembles from multi models are needed. In this way, we can minimize uncertainties of the projection.

5. Conclusions

The changes in the mid-summer SAT and associated internal variability over China at 1.5 °C and 2 °C global warming are examined by analyzing the outputs from the MPI-ESM Grand Ensemble simulations. The results indicate that the additional 0.5 °C of global warming results in an increase of 0.9 °C in the mid-summer SAT over China, which is stronger than the annual SAT (0.8 °C). As a result, every other mid-summer in 1.5 °C global warming and every mid-summer in 2 °C global warming would be hotter than the observed hottest record in 2018.

At the regional scale, in a 1.5 °C and 2 °C global warming, the increases in mid-summer SAT are stronger towards the northwest. In particular, the regional averaged mid-summer SAT over western Northwest China and eastern Northwest China is expected to increase by 1.3 °C and 1.1 °C from 1.5 °C to 2 °C global warming, respectively. The result suggests that more than half of the relatively hotter mid-summers over western China, even 70% over western Northwest China, in 2 °C global warming could be avoided by limiting global warming to 1.5 °C.

There are significant regional differences in the changes in mid-summer SAT internal variability over China from 1.5 °C to 2 °C global warming. Due to an additional 0.5 °C global warming, the internal variability in mid-summer SAT decreases over North China, Northeast China and the western parts of western Northwest China and Tibetan Plateau, while it increases over other regions. Specifically, in Qinghai, Inner Mongolia, and Sichuan provinces, a more notable increase in internal variability would cause more extremely hot mid-summers in 2 °C global warming. Furthermore, due to an additional 0.5 °C global warming, the extremely high monthly SAT for events with return periods of 20 and 100 years would increase nationwide, with Qinghai and Xinjiang provinces have the strongest increases.

Declaration of competing interest

No conflict of interest exits in the submission of this manuscript, and manuscript is approved by all authors for publication.

Acknowledgments

This research was supported by the National Key R&D Program of China (2017YFA0603802), the National Natural Science Foundation of China (41661144005 and 41822502), and the JPI Climate-Belmont Forum project InterDec. We also acknowledge the group in the Max Planck institute for Meteorology that produced the MPI-ESM Grand Ensemble simulations (https://www.mpimet.mpg.deen/grand-ensemble).

References

Chen, H.P., Sun, J.Q., 2018. Projected changes in climate extremes in China in a 1.5°C warmer world. Int. J. Climatol. 38, 3607−3617.
Chen, H.P., Sun, J.Q., 2019. Increased population exposure to extreme droughts in China due to 0.5 °C of additional warming. Environ. Res. Lett. 14, 064011.
Chen, J., Dai, A., Zhang, Y., 2019. Projected changes in daily variability and seasonal cycle of near-surface air temperature over the globe during the Twenty-First century. J. Clim. 32, 8537−8561.
Chen, R.D., Wen, Z.P., Lu, R.Y., 2016. Evolution of the circulation anomalies and the Quasi-Biweekly Oscillations associated with extreme heat events in Southern China. J. Clim. 29, 6909−6921.
Chen, X.C., Xu, Y., Yao, Y., 2015. Changes in climate extremes over China in a 2 °C, 3 °C, and 4 °C warmer world. Chin. J. Atmos. Sci. 39, 1123−1135.
Díaz, J., García, R., De Castro, F.V., et al., 2002. Effects of extremely hot days on people older than 65 years in Seville (Spain) from 1986 to 1997. Int. J. Biometeorol. 46, 145−149.
Ding, Y.G., Liu, J.F., Zhang, Y.C., 2004. Simulation tests of temporal-spatial distributions of extreme temperatures over China based on Probability Weighted Moments estimation. Chin. J. Atmos. Sci. 28, 771−782.
Dosio, A., Mentaschi, L., Fischer, E.M., et al., 2018. Extreme heat waves under 1.5 °C and 2 °C global warming. Environ. Res. Lett. 13, 054006.
Fu, C.B., Qian, C., Wu, Z.H., 2011. Projection of global mean surface air temperature changes in next 40 years: uncertainties of climate models and an alternative approach. Sci. China Earth Sci. 54, 1400−1406.
Fu, Y.H., Lu, R.Y., Guo, D., 2018. Changes in surface air temperature over China under the 1.5 and 2.0 °C global warming targets. Adv. Clim. Change Res. 9, 112−119.
Gao, X.J., Wang, M.L., Filippo, G., 2013. Climate change over China in the 21st century as simulated by BCC_CSM1.1-RegCM4.0. Atmos. Oceanogr. Sci. Libr. 6, 381−386.
Gosling, S.N., Lowe, J.A., McGregor, G.R., et al., 2008. Associations between elevated atmospheric temperature and human mortality: a critical review of the literature. Climatic Change 92, 299−341.

Hansen, J., Sato, M., Ruedy, R., et al., 2006. Global temperature change. Proc. Natl. Acad. Sci. Unit. States Am. 103, 14288−14293.
Hansen, J., Ruedy, R., Sato, M., et al., 2010. Global surface temperature change. Rev. Geophys. 48, RG4004.
He, D.X., 2017. Quantitative analysis on the effects of extreme climate on gain production in China. Chin. J. Agri. Res. Reg. Plan. 38, 28−34.
Hou, W., Chen, Y., Li, Y., et al., 2014. Climatic characteristics over China in 2013. Meteorol. Mon. 40, 491−501.
Howitt, R., Medellín-Azuara, J., MacEwan, D., et al., 2014. Economic Analysis of the 2014 Drought for California Agriculture. Center for Watershed Sciences, University of California, Davis.
Hu, T., Sun, Y., Zhang, X.B., 2017. Temperature and precipitation projection at 1.5 and 2°C increase in global mean temperature. Chin. Sci. Bull. 62, 3098−3111.
IPCC, 2012. Managing the risks of extreme events and disasters to advance climate change adaptation. A Special Report of Working Groups I and II of the Intergovernmental Panel on Climate Change. Cambridge University Press, Cambridge and New York.
Jiang, D.B., Fu, Y.H., 2012. Climate change over China with a 2°C global warming. Chin. J. Atmos. Sci. 36, 234−246.
Jiang, D.B., Wang, H.J., Lang, X.M., 2004. Multimodel ensemble prediction for climate change trend of China under SRES A2 scenario. Chin. J. Geophys. 47, 878−886.
Jiang, D.B., Zhang, Y., Sun, J.Q., 2009. Ensemble projection of 1−3 °C warming in China. Chin. Sci. Bull. 54, 3326−3334.
Jiang, D.B., Sui, Y., Lang, X.M., 2016. Timing and associated climate change of a 2 °C global warming. Int. J. Climatol. 36, 4512−4522.
Joshi, M., Hawkins, E., Sutton, R., et al., 2011. Projections of when temperature change will exceed 2 °C above pre-industrial levels. Nat. Clim. Change 1, 407−412.
Karmalkar, A.V., Bradley, R.S., 2017. Consequences of global warming of 1.5 °C and 2 °C for regional temperature and precipitation changes in the Contiguous United States. PloS One 12, e0168697.
Kennedy, J.J., Thorne, P.W., Peterson, T.C., et al., 2010. How do we know the world has warmed? Bull. Am. Meteorol. Soc. 91, S26−S27.
King, A.D., Karoly, D.J., 2017. Climate extremes in Europe at 1.5 and 2°C of global warming. Environ. Res. Lett. 12, 114031.
King, A.D., Karoly, D.J., Henley, B.J., 2017. Australian climate extremes at 1.5°C and 2°C of global warming. Nat. Clim. Change 7, 412−416.
Kilbourne, E.M., 1997. Heat waves and hot environments. In: Noji, E.K. (Ed.), The Public Health Consequences of Disasters. Oxford University Press, Oxford, pp. 245−269.
Knutti, R., Allen, M.R., Friedlingstein, P., et al., 2008. A review of uncertainties in global temperature projections over the twenty-first century. J. Clim. 21, 2651−2663.
Kuang, X., Zhang, Y., Wang, Z., et al., 2019. Characteristics of boreal winter cluster extreme events of low temperature during recent 35 years and its future projection under different RCP emission scenarios. Theor. Appl. Climatol. 138, 569−579.
Kjellstrom, T., Crowe, J., 2011. Climate change, workplace heat exposure, and occupational health and productivity in Central America. Int. J. Occup. Environ. Health 17, 270−281.
Lang, X.M., Sui, Y., 2013. Changes in mean and extreme climates over China with a 2 °C global warming. Chin. Sci. Bull. 58, 1453−1461.
Li, D.H., Zhou, T.J., Zou, L.W., et al., 2018a. Extreme high-temperature events over East Asia in 1.5°C and 2°C warmer futures: analysis of NCAR CESM low-warming experiments. Geophys. Res. Lett. 45, 1541−1550.
Li, W., Jiang, Z.H., Zhang, X.B., et al., 2018b. Additional risk in extreme precipitation in China from 1.5 °C to 2.0 °C global warming levels. Sci. Bull. 63, 228−234.
Li, Y., Zeng, H.L., Wang, G.F., et al., 2020. Climatic characteristics and major meteorological events over China in 2019. Meteorol. Mon. 46, 547−555.
Miao, J.P., Wang, T., Chen, D., 2020. More robust changes in the East Asian winter monsoon from 1.5 to 2.0 °C global warming targets. Int. J. Climatol. 1−19.
Mitchell, D., James, R., Forster, P.M., et al., 2016. Realizing the impacts of a 1.5 °C warmer world. Nat. Clim. Change 6, 735−737.
Qian, W.H., Lu, B., Zhu, C.W., 2010. How would global-mean temperature change in the 21st century? Chin. Sci. Bull. 55, 1963−1967.
Qin, D.H., Zhang, J.Y., Shan, C.C., Song, L.C., 2015. China National Assessment Report on Risk Management and Adaptation of Climate Extremes and Disasters, refined edition. Science Press, Beijing.
Robine, J.M., Cheung, S.L., Le Roy, S., et al., 2008. Death toll exceeded 70,000 in Europe during the summer of 2003. C. R. Biologies. 331, 171−178.
Rogelj, J., Knutti, R., 2016. Geosciences after Paris. Nat. Geosci. 9, 187−189.
Schleussner, C.F., Rogelj, J., Schaeffer, M., et al., 2016. Science and policy characteristics of the Paris Agreement temperature goal. Nat. Clim. Change 6, 827−835.
Schneider, S.H., Semenov, S., Patwardhan, A., et al., 2007. Assessing key vulnerabilities and the risk from climate change. In: IPCC, Climate Change 2007: Impacts, Adaptation and Vulnerability. Contribution of Working Group II to the Fourth Assessment Report of the Intergovernmental Panel on Climate Change. Cambridge University Press, Cambridge, pp. 779−810.
Shi, C., Jiang, Z.H., Chen, W.L., et al., 2018. Changes in temperature extremes over China under 1.5 °C and 2 °C global warming targets. Adv. Clim. Change Res. 9, 120−129.
Suárez-Gutiérrez, L., Li, C., Müller, W.A., et al., 2018. Internal variability in European summer temperatures at 1.5°C and 2°C of global warming. Environ. Res. Lett. 13, 064026.
Sun, C., Jiang, Z., Li, W., et al., 2019. Changes in extreme temperature over China when global warming stabilized at 1.5°C and 2.0°C. Sci. Rep. 9, 14982.
Sun, Y., Zhang, X., Zwiers, F.W., et al., 2014. Rapid increase in the risk of extreme summer heat in Eastern China. Nat. Clim. Change 4, 1082−1085.
Sutton, R.T., Dong, B., Gregory, J.M., 2007. Land/sea warming ratio in response to climate change: IPCC AR4 model results and comparison with observations. Geophys. Res. Lett. 34, L02701.
Su, Y.N., He, Y.L., Ma, R., et al., 2018. The impact of hot weather on labor productivity in the context of climate change. J. Environ. Hyg. 8, 399−405.
Swain, D.L., Tsiang, M., Haugen, M., et al., 2014. The extraordinary California drought of 2013/2014 character, context, and the role of climate change. Bull. Am. Meteorol. Soc. 95, S3−S7.
Thorne, P., 2015. Briefing: how do we know the globe has warmed? What do we know about why? Proc. Insti. Civ. Eng. Forensic Eng. 168, 58−64.
Trenberth, K.E., Jones, P.D., Ambenje, P., et al., 2007. Observations: surface and atmospheric climate change. In: IPCC, Climate Change 2007: the Physical Science Basis. Contribution of Working Group I to the Fourth Assessment Report of the Intergovernmental Panel on Climate Change. Cambridge University Press, Cambridge and New York, pp. 236−336.
UNFCCC (United Nations Framework Convention on Climate Change), 2015. Adoption of the Paris Agreement, Geneva.
Wang, G.L., Yang, P.C., 2014. Projections of global mean surface temperature under future emissions scenarios using a new predictive technique. Atmos. Oceanogr. Sci. Libr. 7, 186−189.
Wang, S.W., Luo, Y., Zhao, Z.C., et al., 2013. Global mean temperature has risen by 1°C since the industrialization. Adv. Clim. Change Res. 9, 383−385.
Wang, T., Miao, J.P., Sun, J.Q., et al., 2018a. Intensified East Asian summer monsoon and associated precipitation mode shift under the 1.5 °C global warming target. Adv. Clim. Change Res. 9, 102−111.
Wang, X.X., Jiang, D.B., Lang, X.M., 2018b. Climate change of 4 °C global warming above pre-industrial levels. Adv. Atmos. Sci. 35, 757−770.
Wang, Y., Zhou, B., Qin, D., et al., 2017a. Changes in mean and extreme temperature and precipitation over the arid region of northwestern China: observation and projection. Adv. Atmos. Sci. 34, 289−305.
Wang, Z.L., Lin, L., Zhang, X.Y., et al., 2017b. Scenario dependence of future changes in climate extremes under 1.5°C and 2°C global warming. Sci. Rep. 7, 46432.
Wehner, M., Stone, D., Mitchell, D., et al., 2018. Changes in extremely hot days under stabilized 1.5 and 2.0 °C global warming scenarios as simulated by the HAPPI multi-model ensemble. Earth. Syst. Dyn. 9, 299−311.

Williams, A.P., Seager, R., Abatzoglou, J.T., et al., 2015. Contribution of anthropogenic warming to California drought during 2012−2014. Geophys. Res. Lett. 42, 6819−6828.

Wu, J., Gao, X.J., 2013. A gridded daily observation dataset over China region and comparison with the other data sets. Chin. J. Geophys. 56, 1102−1111.

Xu, C.H., Xu, Y., 2012. The projection of temperature and precipitation over China under RCP scenarios using a CMIP5 multi-model ensemble. Atmos. Oceanogr. Sci. Libr. 5, 527−533.

Xu, K., Lu, R., Mao, J., et al., 2019. Circulation anomalies in the mid−high latitudes responsible for the extremely hot summer of 2018 over northeast Asia. Atmos. Oceanogr. Sci. Libr. 12, 231−237.

Xu, Y., Zhao, Z.C., Luo, Y., et al., 2005. Climate change projections for the 21st century by the NCC/IAP T63 model with SRES scenarios. Acta Meteorol. Sin. 19, 407−417.

Xu, Y., Zhou, B.T., Wu, J., et al., 2017. Asian climate change under 1.5−4 °C warming targets. Adv. Clim. Change Res. 8, 99−107.

Xu, Y., Gao, X.J., Giorgi, F., et al., 2018. Projected changes in temperature and precipitation extremes over China as measured by 50-yr return values and periods based on a CMIP5 ensemble. Adv. Atmos. Sci. 35, 376−388.

Yao, S.B., Jiang, D.B., Fan, G.Z., 2017. Seasonality of precipitation over China. Chin. J. Atmos. Sci. 41, 1191−1203.

Yu, B., Li, G.L., Chen, S.F., et al., 2020. The role of internal variability in climate change projections of North American surface air temperature and temperature extremes in CanESM2 large ensemble simulations. Clim. Dynam. 55, 869−885.

Yu, S., Xia, J.J., Yan, Z.W., et al., 2019. Loss of work productivity in a warming world: differences between developed and developing countries. J. Clean. Prod. 20, 1219−1225.

Zhai, P.M., Yu, R., Zhou, B.Q., et al., 2017. Research progress in impact of 1.5°C Global warming on Global and regional scales. Clim. Change Res. 13, 465−472.

Zhang, G.W., Zeng, G., Iyakaremye, V., et al., 2020. Regional changes in extreme heat events in China under stabilized 1.5°C and 2.0°C global warming. Adv. Clim. Change Res. 11 (3), 198−209. https://doi.org/10.1016/j.accre.2020.08.003.

Zhang, L., Ding, Y.H., Wu, T.W., et al., 2013. The 21st century annual mean surface air temperature change and the 2°C warming threshold over the globe and China as projected by the CMIP5 models. Acta Meteorol. Sin. 71, 1047−1060.

Zhang, Q., Zhao, Y.X., Wang, C.Y., 2011. Study on the impact of high temperature damage rice in the lower and middle reaches of Yangtze river. J. Catastrophol. 26, 57−62.

Zhang, X.L., Wang, Y.C., 2002. Relationship between power consumption and meteorological conditions during the summer in Beijing city and its forecast. Meteorol. Mon. 28, 17−21.

Zhang, Y., 2012. Projections of 2.0 °C warming over the globe and China under RCP4.5. Atmos. Oceanogr. Sci. Libr. 5, 514−520.

Zhou, B.T., Wen, Q.Z.H., Xu, Y., et al., 2014. Projected changes in temperature and precipitation extremes in China by the CMIP5 multimodel ensembles. J. Clim. 27, 6591−6611.

Zhou, B.T., Xu, Y., Wu, J., et al., 2016a. Changes in temperature and precipitation extreme indices over China: analysis of a high-resolution grid dataset. Int. J. Climatol. 36, 1051−1066.

Zhou, L.M., Chen, H.S., Dai, Y.J., 2015. Stronger warming amplification over drier ecoregions observed since 1979. Environ. Res. Lett. 10, 064012.

Zhou, L.M., Chen, H.S., Hua, W.J., et al., 2016b. Mechanisms for stronger warming over drier ecoregions observed since 1979. Clim. Dynam. 47, 2955−2974.

Zhou, M.Z., Zhou, G.S., Lü, X.M., et al., 2019a. Projection of temperature and precipitation changes over China under global warming of 1.5 and 2°C. Acta Meteorol. Sin. 77, 728−744.

Zhou, X.Y., Zeng, H.L., Wang, Z.Y., et al., 2019b. Climatic characteristics and major meteorological events over China in 2018. Meteorol. Mon. 45, 543−552.

Zou, H.B., Wu, S.S., Shan, J.S., et al., 2015. Diagnostic study of the severe high temperature event over Mid-East China in 2013 summer. Acta Meteorol. Sin. 73, 481−495.